Anticancer effects of KI-10F: A novel compound affecting apoptosis, angiogenesis and cell growth in colon cancer

SANG-WON HONG[1,2], KYUNG HEE JUNG[1], MYUNG-JOO CHOI[1], DA YOUNG KIM[1], HEE-SEUNG LEE[1], HONG-MEI ZHENG[1], GUANG YONG LI[1], IBRAHIM M. EL-DEEB[3], BYUNG SUN PARK[3], SO HA LEE[3] and SOON-SUN HONG[1]

[1]NCEED and Department of Biomedical Sciences, College of Medicine, Inha University, Incheon 400-712, Republic of Korea; [2]School of Biology and Parker H. Petit Institute of Bioengineering and Biosciences, Georgia Institute of Technology, Atlanta, GA 30332, USA; [3]Chemical Kinomics Research Center, Korea Institute of Science and Technology, Seoul 130-650, Republic of Korea

Received May 24, 2012; Accepted July 27, 2012

DOI: 10.3892/ijo.2012.1609

Abstract. The anticancer effect of a new pyrazole derivative, KI-10F (2-(4-(2-(4-(dimethylamino) phenyl)pyridin-4-yl)-5-(3-methoxy-5-methylphenyl)-1H-pyrazol-1-yl) acetonitrile)•3.5HCl) was evaluated in human colon cancer cells. KI-10F strongly suppressed the growth of human colon cancer cells and induced apoptosis by increasing the proportion of sub-G1 presenting apoptotic cells as well as causing cell cycle arrest at the G2/M phase. Apoptosis by KI-10F was confirmed by observation of an increase in the expression of cleaved caspase-3, caspase-8, caspase-9 and Bax, and the decrease of Bcl-2. Decreased expression of HIF-1α and VEGF, and the inhibition of HUVEC tube formation and migration showed that KI-10F effectively inhibited the angiogenesis process. Furthermore, *in vivo* study in a mouse xenograft model showed that KI-10F produced a stronger antitumor activity than 5-FU, a conventional anticancer drug prescribed for the treatment of colon cancer. The effects of KI-10F on tumor proliferation (PCNA), angiogenesis (CD34) and apoptosis (cleaved caspase-3) were evaluated by immunohistochemistry using isolated tumor tissue samples. Taken together, our results demonstrated that KI-10F induces apoptosis and inhibits cell growth and angiogenesis both *in vitro* and *in vivo*. We suggest that KI-10F is an effective chemotherapeutic candidate for use against colon cancer.

Correspondence to: Dr Soon-Sun Hong, NCEED and Department of Biomedical Sciences, College of Medicine, Inha University, 3-ga, Sinheung-dong, Jung-gu, Incheon 400-712, Republic of Korea
E-mail: hongs@inha.ac.kr

Dr So Ha Lee, Chemical Kinomics Research Center, Korea Institute of Science and Technology, Seoul 130-650, Republic of Korea
E-mail: lsh6211@kist.re.kr

Key words: cell cycle, angiogenesis, apoptosis, colon cancer

Introduction

Colon cancer is one of the leading causes of cancer related death worldwide with over 500,000 deaths every year and its incidence continues to rise in the eastern world (1). There are many possible causes of colon cancer including advanced age, smoking, diet, environmental factors, exogenous hormones like estrogens, polyps of the colons, family history (genetic predisposition), familial adenomatous polyposis (FAP), hereditary nonpolyposis colorectal cancer (HNPCC), Lynch syndrome, long-standing ulcerative colitis, and Crohn's disease of the colon (2). In its early stage, surgery can be an effective primary treatment, but surgical resection is unsatisfactory in cases of metastasis and reoccurrence (3). Thus other treatment options such as chemotherapeutic agents have been introduced, and 5-flurouracil (5-FU) remains a widely used first-line colon cancer treatment in patients over 50 years of age (4). However there are inter-individual differences in response, survival and toxicity in patients treated with 5-FU (5). Developing new anticancer agents for use in treatment against colon cancer are needed in order to provide reliable treatment for patients.

Several pyrazole derivatives have been reported to have a wide range of biological activities such as antitumor, antibacterial, anti-inflammatory, analgesic, and fungistatic activity (6-9). So, they are increasingly gaining interest as important compounds in the pharmaceutical industry and medicinal chemistry. Of these, anticancer activities have been the most studied. Especially, pyrazole derivatives induce apoptosis and inhibition of angiogenesis in cancers (10,11). In addition, pyridine derivatives have been reported to possess anticancer effect such as inhibition of cell growth, induction of cell cycle arrest, and apoptosis without cytotoxicity in various cancer cells (12,13). On the basis of previous finding, we have synthesized a new active pyrazole and pyridine derivatives, culminating in the discovery of 2-(4-(2-(4-(dimethylamino) phenyl) pyridin-4-yl)-5-(3-methoxy-5-methylphenyl)-1H-pyrazol-1-yl) acetonitrile)•3.5HCl) (Fig. 1, designated KI-10F).

One of the hallmarks of cancer cells including colon cancer is uncontrolled cell proliferation and escape of apoptosis

by cancer cells. Especially, angiogenesis plays an important role in the progression of cancer and correlates with higher incidences of metastasis and poor prognosis in human colon cancers (14). The presence of microvessels and the vascular endothelial growth factor (VEGF) are significantly involved in endothelial cell proliferation, migration, invasion and, tumor recurrence (15). Also, apoptosis and proliferation imbalance leads to malignant transformation and tumorigenesis of normal tissues (16). Therefore, induction of apoptosis along with inhibiting angiogenesis by non-toxic compounds is a promising strategy for checking the uncontrolled colon cancer cell proliferation and survival.

In this study, therefore, we synthesized a new pyrazole derivative KI-10F and assessed its possibility as a chemotherapeutic agent against colon cancer. Our results showed that KI-10F induced apoptosis and inhibited angiogenesis *in vitro* and *in vivo*.

Materials and methods

Cells and materials. The human colon cancer cell lines HT-29, LoVo, RKO and human umbilical vein endothelial cells (HUVECs) were purchased from ATCC (Manassas, VA). The HT-29 cells were cultured in Roswell Park Memorial Institute Media 1640 (RPMI-1640) and the LoVo and RKO cells were cultured in Dulbecco's modified Eagle's medium (DMEM), supplemented with 10% fetal bovine serum (FBS) and 1% penicillin/streptomycin. The HUVECs were grown in a gelatin coated flask in M199 medium containing 20 ng/ml of basic fibroblast growth factor (bFGF), 100 U/ml heparin and 20% FBS. The cell cultures were maintained at 37˚C in a CO_2 incubator with a controlled humidified atmosphere composed of 95% air and 5% CO_2. The FBS, cell culture media, penicillin-streptomycin, and all other agents used in the cell culture studies were purchased from Invitrogen.

Synthesis of KI-10F. 2-(4-(2-(4-(Dimethylamino)phenyl) pyridin-4-yl)-5-(3-methoxy-5-methylphenyl)-1H-pyrazol-1-yl) acetonitrile (700 mg, 1.65 mM) in hydrogen chloride solution (5 ml, 5 mM, 1 M/diethyl ether) was vigorously stirred for 30 min, and then filtered to collect the solid which was washed with hexane to give the pure KI-10F as a yellow solid. Yield: 750 mg; mp 125-128˚C; ^{1}H NMR (300 MHz, D_2O) δ (ppm) 2.19 (s, 3H), 2,98 (sec, 6H), 3.64 (s, 3H), 5.07 (s, 2H), 6.53 (s, 1H), 6.62 (s, 1H), 7.01 (s, 1H), 7.07 (d, J=8.7 Hz, 2H), 7.24 (d, J=8.7 Hz, 2H), 7.31 (s, 1H), 7.42 (d, J=6.3 Hz, 1H), 8.14 (d, J=4.8 Hz, 2H); elemental analyses ($C_{26}H_{28.5}Cl_{3.5}N_5O$) calcd: C, 56.66; H, 5.21; N, 12.71. Found: C, 56.64; H, 5.63; N, 12.60.

Measurement of cell proliferation. Cell viability analysis was performed using the MTT (3-(4,5-dimethylthiazol-2-yl)-2,5-diphenyltetrazolium bromide) assay. Briefly, the HT-29, LoVo, and RKO cells were plated at a density of $1x10^4$ cells/well in 96-well plates and incubated for 24 h. The medium was removed, and the cells were treated with either D.W. as a control or various concentrations (0.01, 0.05, 0.1, 0.5, 1 or 5 μM) of KI-10F or 5-FU. After the cells were incubated for an additional 48 h, 20 μl of MTT solution (2 mg/ml) was added to each well and they were incubated for another 4 h at 37˚C. After removing the media, the formed formazan crystals were dissolved in DMSO (200 μl/well) by constant shaking for 5 min. The plate was then read on a microplate reader at 540 nm. Three replicate wells were used for each analysis. The median inhibitory concentration (IC_{50}, defined as the drug concentration at which cell growth was inhibited by 50%) was assessed from the dose-response curves.

Western blot analysis. Cells were washed with ice-cold phosphate-buffered saline (PBS) before lysis. The cells were lysed with buffer containing 1% Triton X-100, 1% Nonidet P-40, and the following protease and phosphatase inhibitors: aprotinin (10 mg/ml), leupeptin (10 mg/ml) (ICN Biomedicals, Asse-Relegem, Belgium), phenylmethylsulfonyl fluoride (1.72 mM), NaF (100 mM), $NaVO_3$ (500 mM), and $Na_4P_2O_7$ (500 mg/ml) (Sigma-Aldrich). Protein (50 μg) was separated from the mixture using 10% sodium dodecyl sulfate-polyacrylamide (SDS) gel electrophoresis, it was then transferred onto nitrocellulose membranes and evaluated using Ponceau S solution staining (Sigma-Aldrich). Immunostaining of the blots was performed using the primary antibodies followed by the secondary antibody conjugated to horseradish peroxidase with detection using enhanced chemiluminescence reagent (ELPS, Seoul, Korea). The primary antibodies were mouse monoclonal: anticleaved caspase-3, cleaved caspase-8, cleaved caspase-9 (Cell Signaling Technologies, Danvers, MA), Bax and Bcl-2 (Santa Cruz Biotechnology, Santa Cruz, CA), anti-HIF-1α, and anti-β-actin (BD Biosciences, San Jose, CA), and anti-VEGF (Cell Signaling Technologies, Danvers, MA). The secondary antibodies were purchased from Amersham Biosciences. The bands were visualized using the ECL plus system (Amersham Pharmacia Biotech Inc., Piscataway, NJ).

Cell cycle analysis. HT-29 cells were plated in 100-mm diameter culture dishes and then incubated. The next day, the cells were treated with various concentrations (0 to 1 μM) of KI-10F for 24 h. Floating and adherent cells were collected and fixed in 70% ethanol at 4˚C overnight. After washing, the cells were subsequently stained with 50 μg/ml of PI and 100 μg/ml of RNase A for 1 h in the dark and then subjected to flow cytometric analysis in order to determine the percentage of cells at specific cell cycle phase. Flow cytometric analysis was performed using a FACSCalibur flow cytometer (Becton Dickinson, San Jose, CA) equipped with a 488-nm argon laser. Events were evaluated for each sample and the cell cycle distribution was analyzed using Cell Quest software (Becton Dickinson). The results were presented as the number of cells versus the amount of DNA as indicated by fluorescence signal intensity. All the experiments were conducted three times.

DAPI staining and TUNEL assay. The HT-29 cells were plated onto 18-mm cover glasses in RPMI-1640 medium and grown to ~70% confluence for 24 h. The cells were then treated with KI-10F at a dose of 0.5 μM for 24 h. The cells were fixed in 2% ice-cold paraformaldehyde (PFA), washed with PBS and then stained with 2 μg/ml of 4,6-diamidino-2-phenylindole (DAPI) for 20 min at 37˚C. The DAPI stained cells were examined under a fluorescent microscope in order to evaluate any nuclear fragmentation. Terminal deoxynucleotidyl transferase-mediated nick end labeling (TUNEL) was performed following

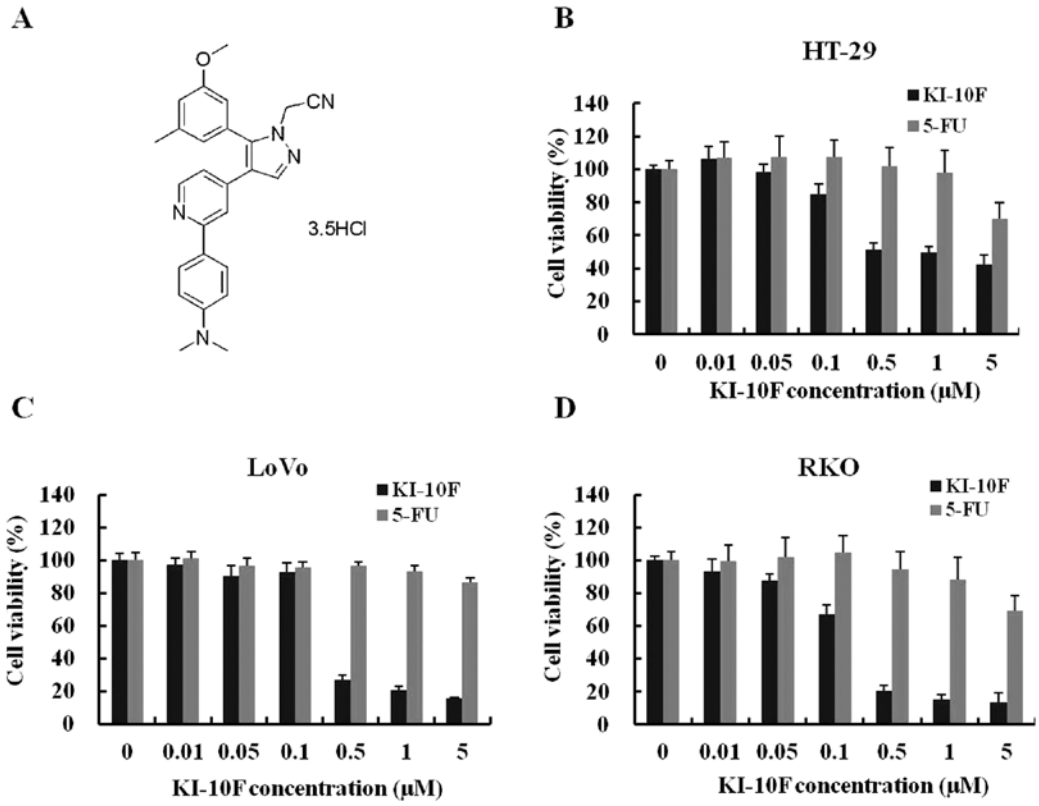

Figure 1. Effect of KI-10F on the proliferation of human colon cancer cells. (A) Chemical structure of KI-10F, 2-(4-(2-(4-(Dimethylamino)phenyl)pyridin-4-yl)-5-(3-methoxy-5-methylphenyl)-1H-pyrazol-1-yl)acetonitrile•3.5HCl. Cytotoxic effects of KI-10F and 5-FU on colon cancer cells, (B) HT-29, (C) LoVo and (D) RKO cells were measured using an MTT assay. Results are expressed as percent cell proliferation relative to the control.

the manufacturer's protocol for the use of the TUNEL kit (Chemicon, Temecula, CA).

HUVEC tube formation assay. Matrigel (200 μl) (10 mg/ml) (BD Biosciences, NJ) was polymerized for 30 min at 37˚C. The HUVECs were suspended in M199 (5% FBS) medium at a density of 2.5x10^5 cells/ml. Then 0.2 ml of cell suspension was added to each Matrigel coated well either with or without the indicated concentrations of KI-10F, and then they were incubated for 14 h. The morphological changes of the cells and HUVEC tube formations were observed under a phase-contrast microscope and photographed at x200 magnification.

HUVEC migration assay. HUVECs, plated on 60 mm diameter culture dishes at 90% confluence, were wounded with a 2 mm razor blade and marked at the injury line. After wounding, the peeled off cells were removed with serum-free medium and further incubated in M199 with 5% serum, 1 mM thymidine (Sigma-Aldrich) and/or KI-10F. The HUVECs were allowed to migrate for 24 h and were then rinsed with serum-free medium followed by fixing with absolute methanol and staining with Giemsa (Sigma-Aldrich). Migration was quantitated by counting the number of cells that moved beyond the reference line.

Tumor xenograft study. Six-week-old male nude mice were obtained from Central Laboratory Animal Inc. (Seoul, Korea). Animal care and all experimental procedures were conducted in accordance with the approval and guidelines of the Inha Institutional Animal Care and Use Committee of the Medical School of Inha University. The animals were fed standard rat chow and tap water *ad libitum*, and were maintained under a 12 h dark/light cycle at 37˚C. The mice were randomly divided into three groups (control, KI-10F at 1 mg/kg and 5-FU at 10 mg/kg). The HT-29 cells were harvested, mixed with PBS (200 μl/mouse) and then inoculated into one flank of each nude mouse (2x10^6 of HT-29 cells). When the tumor volume reached ~50-100 mm^3, the mice were orally administered either KI-10F (1 mg/kg), 5-FU (10 mg/kg, positive control group) or the vehicle (200 μl of 0.7% CMC, control group) three times per week for 3 weeks. The tumor dimensions were measured twice a week using a digital caliper and the tumor volume was calculated using the formula: V = length x $width^2$ x 0.5. At the end of the experiment, the mice were sacrificed, and the tumors were excised and weighed. A portion of each tumor was fixed in buffered formalin and then embedded in paraffin. The remaining tissue was stored at -70˚C for further analysis.

Immunohistochemistry in the tumor tissue. After deparaffinization, immunostaining was performed on 8-μm thick sections of tumor tissue. Microwave antigen retrieval was performed in citrate buffer (pH 6.0) for 10 min prior to peroxidase quenching with 3% H_2O_2 in PBS for 10 min. The sections were then washed in water and preblocked with normal goat or horse serum for 10 min. Next, the tissue sections were incubated overnight at 4˚C in 1:50 dilutions of mouse anticleaved caspase-3 (Cell Signaling), anti-PCNA and anti-CD34 antibodies (Santa Cruz Biotechnology). The sections were then incubated with biotinylated secondary antibodies (1:200) for 1 h. Following a washing

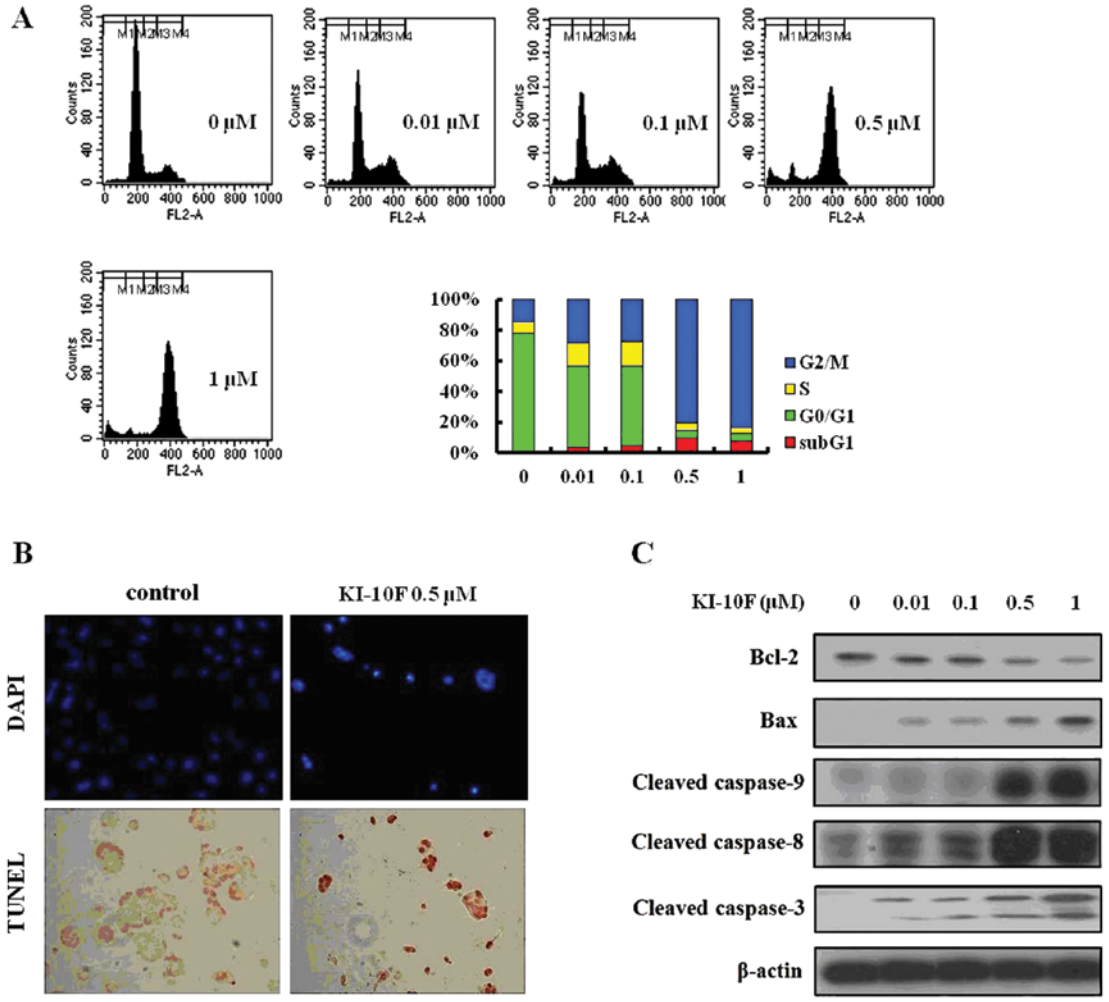

Figure 2. Effect of KI-10F on cell cycle distribution and apoptosis in HT-29 cells. (A) HT-29 cells were treated with KI-10F (0.01-1 μM) for 48 h, stained with propidium iodide (PI) and then analyzed on a FACSCalibur flow cytometer. M1, sub-G1; M2, G0/G1; M3, S; M4, G2/M. Quantitation of the PI staining data is presented as the percentages of cell cycle distribution. The induction of apoptosis by KI-10F was evaluated by western blot analysis. (B) The induction of apoptosis by KI-10F was assessed by TUNEL and DAPI staining, the results of which were photographed at x200 magnification. (C) Bcl-2, Bax and cleaved caspase-3, -8 and -9 expression in the cells treated with KI-10F at the indicated doses for 48 h.

step with PBS, streptavidin-HRP was applied. Finally, the sections were developed with diaminobenzidine tetrahydrochloride substrate for 10 min, and counterstained with hematoxylin. At least three random fields of each section were examined at a magnification, x200 and analyzed by a computer image analysis system (Media Cybernetics, Silver Spring, MD).

Statistical analysis. Data are expressed as mean ± SD. Statistical analysis was performed using ANOVA and an unpaired Student's t-test. A p-value ≤0.05 was considered statistically significant. Statistical calculations were performed using SPSS software for the Windows operating system (Version 10.0; SPSS, Chicago, IL).

Results

KI-10F inhibited proliferation of human colon cancer cells. In order to determine the effectiveness of KI-10F on cell growth inhibition, we tested the MTT assay on three colon cancer cell lines (HT-29, LoVo and RKO). The human colon cancer cells were exposed to various concentrations of KI-10F and 5-FU, ranging from 0 to 5 μM, for 48 h. Our results showed that the cell growth was inhibited strongly by KI-10F in a dose-dependent manner as compared with 5-FU, a commercially available drug (Fig. 1). The IC_{50} values of KI-10F administration in the three colon cancer cells were very low (HT-29; 0.30 μM, LoVo; 0.59 μM, RKO; 0.33 μM) whereas 5-FU was unable to inhibit 50% cell proliferation at the highest dose (5 μM). The HT-29 cells were the most sensitive to KI-10F and had the lowest IC_{50} value to KI-10F mediated inhibition of cancer cell growth and proliferation, and were thus chosen for further experiments.

The effects of KI-10F on cell cycle and apoptosis in HT-29 cells. The cell cycle profile induced by KI-10F was measured using flow cytometry. The cells were harvested 48 h after treatment of KI-10F at various concentrations and analyzed for their cell cycle distributions (sub-G1, G0/G1, S and G2/M). Treatment with KI-10F increased the occurrence of the sub-G1 phase and significantly blocked the G2/M phase. At a dose of 0.5 μM, KI-10F rapidly increased the occurrence of the sub-G1 phase by 7.8-fold and G2/M phase by 5.5-fold as compared to the control (0 μM) (Fig. 2A). In order to identify the apoptotic effect of

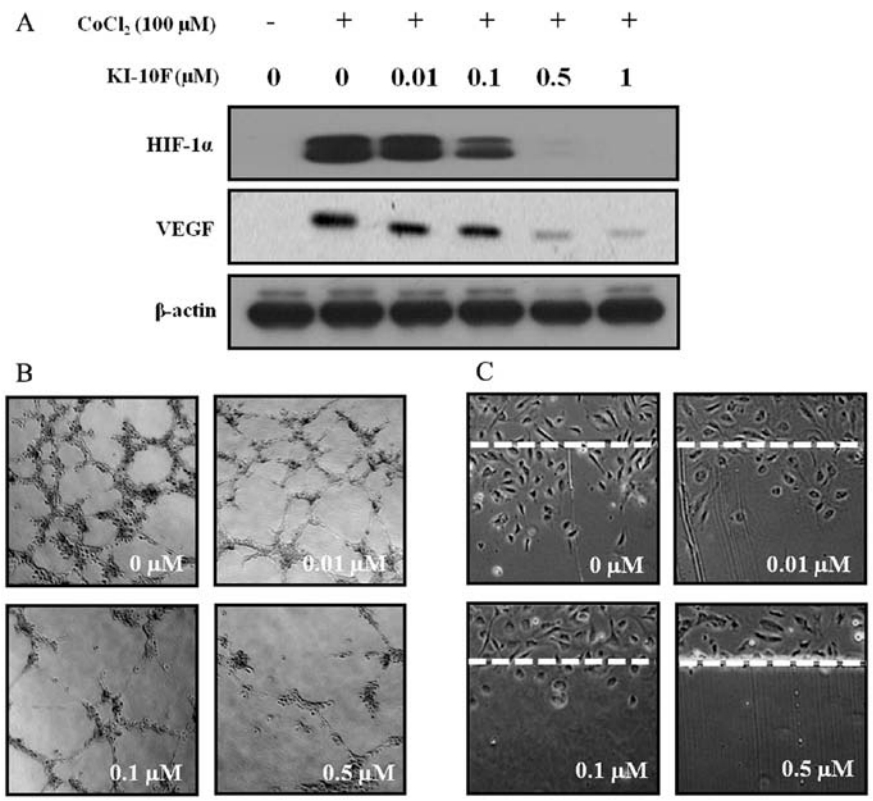

Figure 3. Effect of KI-10F on angiogenesis. (A) Expression of HIF-1α and VEGF by KI-10F in the hypoxia-induced HT-29 cells ($CoCl_2$, 100 μM). (B) Effects of KI-10F on tube formation in the HUVECs. HUVECs were plated on Matrigel (200 μl/well) and treated with various concentrations of KI-10F. Capillary tube formation was assessed after 14 h. Tube formation was observed under a phase-contrast microscope and photographed at x400 magnification. (C) Effects of KI-10F on migration *in vitro*. HUVECs were plated at 90% confluence and a scratch was made with a razor blade. After wounding, the cells were incubated in M199 with 5% FBS, 5 ng/ml bFGF, 1 mM thymidine and/or KI-10F (1 μg/ml). Data represent the mean of at least three independent experiments performed in triplicate.

KI-10F in the HT-29 cells, we performed analysis using DAPI and TUNEL staining. When the HT-29 cells were treated with KI-10F (0.5 μM), the cells presented apoptotic morphological features such as bright nuclear condensation, DNA fragmentation and perinuclear apoptotic bodies visible by DAPI and TUNEL staining (Fig. 2B). In results of western blot analysis, KI-10F dosing seemed to induce apoptosis in the HT-29 cells, whereas it decreased the expression of Bcl-2 and increased the expression of Bax, induced extrinsic apoptosis by activation of the caspase-3, caspase-8 and caspase-9 cascades (Fig. 2C).

The effects of KI-10F dosing on angiogenesis. HIF-1α is a major transcriptional modulator of angiogenic factors such as VEGF. In order to identify the effect of KI-10F on angiogenesis, HT-29 cells were treated with various concentration of KI-10F for 6 h under hypoxia mimic conditions induced by $CoCl_2$ (100 μM), after which we examined the cellular expression of HIF-1α and VEGF using western blot analysis. As shown in Fig. 3A, HIF-1α was highly induced under the hypoxia mimic conditions. However, the expression of HIF-1α and VEGF decreased in a dose-dependent manner. Next, we performed an *in vitro* tube formation assay in order to identify the anti-angiogenic effect of KI-10F on HUVECs. The HUVECs, suspended in complete medium (5% FBS) either with or without KI-10F, were seeded onto a Matrigel layer and the process of capillary tube formation was monitored and photographed 14 h post-incubation. We observed that KI-10F administration inhibited the formation of vessel-like structures consisting of the elongation and alignment of the cells (Fig. 3B). Endothelial cell migration supports the formation of blood vessels during tumor growth and metastasis. Thus, we carried out a wound migration assay in order to examine the effect of KI-10F on the migration of HUVECs. When these endothelial cells were wounded and then incubated in media containing 5% FBS and 1 mM thymidine in the presence of KI-10F (100 μg/ml) over a 24 h period, the wound was unable to heal (Fig. 3C).

The effects of KI-10F on proliferation, angiogenesis, and apoptosis in xenograft model. We next examined the *in vivo* anticancer activity of KI-10F in an HT-29 cell xenograft model using nude mice. There was no difference in body weight change in the KI-10F treated group as compared to the control group (Fig. 4B). This indicated that KI-10F has low toxicity at the curative dose. As shown in Fig. 4A, 1 mg/kg treatment of KI-10F for 3 weeks inhibited tumor growth as compared to the negative control. Furthermore, the 1 mg/kg dose of KI-10F was found to suppress tumor growth more than a 10 mg/kg dose of the commercial available colon cancer drug, 5-FU (Fig. 4A). Our results demonstrated the antitumor efficacy of KI-10F against *in vivo* colon cancer in a mouse model without any apparent sign of toxicity.

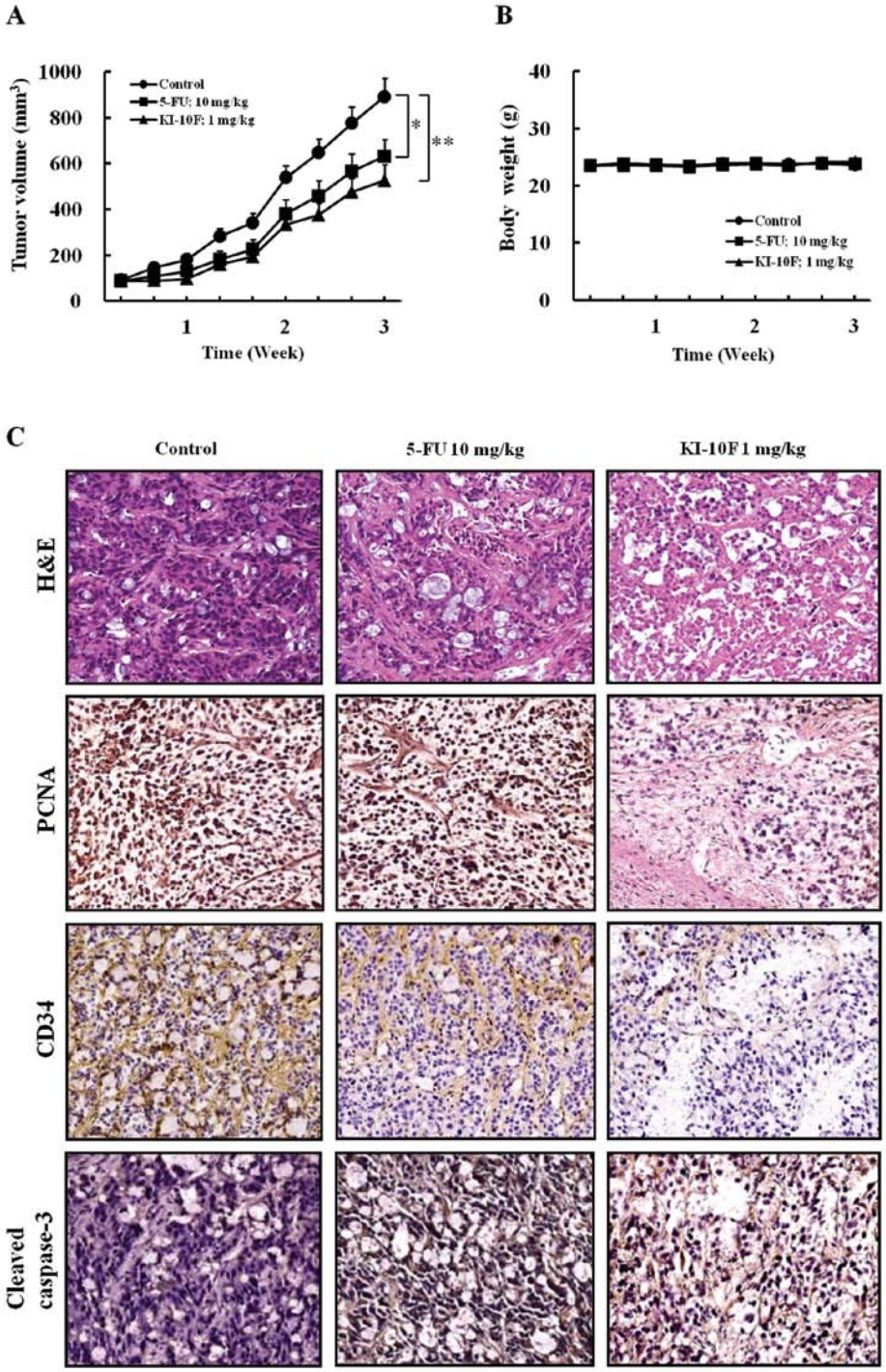

Figure 4. *In vivo* effects of KI-10F using an HT-29 mouse xenograft model. Tumors were implanted into the mice by subcutaneous injection of HT-29 cells ($2x10^6$ cells/200 μl PBS) on the flank. After the tumors reached 50-100 mm^3 in size, the mice received a daily oral administration of KI-10F (1 mg/kg), 5-FU (10 mg/kg) or vehicle (0.7% CMC) for 3 weeks. (A) Tumor volume and (B) body weight changes of the nude mice were measured prior to treatment. (C) Tumors were excised and processed for immunostaining for PCNA, CD34 and cleaved caspase-3 using H&E staining. Original magnification, x200. Data are presented as the mean ± SD (n=10). $^{*}p<0.05$ and $^{**}p<0.01$ vs. control.

Using the results of H&E staining and cleaved caspase-3, we observed that there was a greater degree of tumor apoptosis and necrosis in the KI-10F treated group than in the control group (Fig. 4C). In addition, the IHC results of PCNA showed that administration of KI-10F decreased the proliferation of tumor tissues. Our *in vitro* study showed that KI-10F inhibited angiogenesis and induced apoptosis. Therefore, in order to evaluate the *in vivo* effect of KI-10F on angiogenesis and apoptosis, we investigated CD34 expression. As observed by microscopic analysis, the expression of vessel marker CD34 strongly decreased in the KI-10F treated group as compared to the control group (Fig. 4C). Interestingly, the effects of KI-10F on proliferation, apoptosis and angiogenesis were more potent than that of 5-FU as in the *in vitro* studies.

Discussion

Successfully triggering apoptosis, which causes irreversible death of cancer cells, is an important hallmark for an effective chemotherapeutic agent (17). Angiogenesis is essential to the growth of solid tumors and its inhibition is an effective and promised target for chemotherapeutics. Therefore, in this study we investigated anticancer mechanism of the KI-10F in terms of both apoptosis and anti-angiogenesis. In our previous study, we synthesized various new pyrazole derivatives and from them we selected KI-10F which showed high anticancer activity (18). In this regards, we investigated its possible use as a chemotherapeutic agent against colon cancer cell proliferation, disrupting the cell cycle, promoting apoptosis and inhibiting angiogenesis.

Apoptosis is induced by two alternative pathways, an extrinsic pathway mediated by the death receptor and the intrinsic pathway mediated by mitochondria (19,20). In the intrinsic pathway, mitochondrial apoptosis is initiated by their dysfunction, regulated by the members of the Bcl-2family. Mitochondria activated by proapoptotic Bcl-2 family members (Bax, Bak, Bid, etc.) release cytochrome *c* which binds to apoptotic protease activating factor 1 (APAF1) to form apoptosome in the cytosol (21). Apoptosis through the mitochondrial pathway can be inhibited using anti-apoptotic proteins of the Bcl-2 family (Bcl-2, Bcl-xl, Bcl-w, etc.) (22). In the extrinsic pathway, apoptosis is initiated through the interaction of death receptors located on the cell surface. When a ligand binds to its respective death receptor, initiator caspases are recruited (20,23). Induction of apoptosis leads to activation of the initiator caspases: caspase-8 for the extrinsic pathway and caspase-9 for the intrinsic pathway (20). Once the initiator caspases are activated, they cleave and activate 'executioner' caspases: caspase-3, caspase-6 and caspase-7. Mainly caspase-3 is involved in the process of apoptosis. As apoptosis plays a pivotal role in the prevention of cancer, we investigated the apoptotic effect of KI-10F on HT-29 cells. We observed that KI-10F administration significantly suppressed the colon cancer cell growth in a dose-dependent manner. Treatment by KI-10F induced apoptosis in the HT-29 cells by increasing their expression of cleaved caspase-3, -8 and -9, and Bax. Furthermore, KI-10F dosing decreased the expression of Bcl-2. In the flow cytometry experiment, DNA fragmentation and nuclear condensation were confirmed by an observed increase of cells in the sub-G1 phase. The apoptotic effects of KI-10F were confirmed by the observed DNA fragmentation, nuclear condensation, and cell morphology changes as revealed by TUNEL and DAPI staining. These results implied that the induction of apoptosis by KI-10F may be a contributing factor in their suppression of tumor growth. Cell cycle arrest can trigger proliferation inhibition and apoptosis in cancer cells, and the G2/M checkpoint is a potential target for a cancer agent (24,25). Our cell cycle analysis showed that KI-10F administration strongly induced cell cycle arrest in the G2/M checkpoint.

Inhibition of angiogenesis also can serve as a potential antitumor therapy. Rapid proliferation of cancer cells induces intracellular hypoxia conditions, which in turn initiates the process of the development of new blood vessels (26). In this process, HIF-1α plays an important role by activating transcription of the promoter of VEGF, a key factor in tumor angiogenesis (27). Inhibition of tumor angiogenesis can serve as a potential antitumor therapy because angiogenesis is crucial to tumor growth, invasion and metastasis (28,29). Supporting this point, our *in vitro* studies performed under hypoxia mimic conditions showed that KI-10F inhibited the expression of HIF-1α and VEGF in HT-29 cells. Thus, KI-10F was found to inhibit hypoxia induced angiogenesis. Endothelial cells are the major constituents of new blood vessels whose functioning is the basis of angiogenesis. In the vasculogenesis process, endothelial cells migrate on a matrix, such as collagen, and remodel into tubular structures (30). KI-10F inhibited tube formation and migration of HUVECs. In addition, the *in vivo* anti-angiogenic effect of KI-10F was supported by decreased expression of CD34, a microvessel endothelial cell.

In this study, we investigated the anticancer efficacy and associated mechanisms of KI-10F by studying its effect against colon cancer cells *in vitro*, and then expanded the assessment into an *in vivo* HT-29 xenograft animal model. Our expanded study revealed that KI-10F inhibited cell and tumor growth, and induced apoptosis in both HT-29 cells and the xenograft animal model. In addition, KI-10F suppressed angiogenesis by decreasing the expression of HIF-1α and VEGF in colon cancer cells, and inhibited the vasculogenesis process of endothelial cells. In this regard, it seems that KI-10F has great potential to induce apoptosis and inhibit angiogenesis. Of note, KI-10F at a dose of 1 mg/kg suppressed greater tumor growth than a 10 mg/kg dose of 5-FU, which is the current standard care drug used in patients with advanced colon cancer.

Acknowledgements

This work was supported by the National R&D Program for Cancer Control (1020250), National Center of Efficacy Evaluation for the Development of Health Products Targeting Digestive Disorders (NCEED), Ministry of Health & Welfare, and National Research Foundation of Korea (NRF) funded by the Ministry of Education, Science and Technology (NRF 2012-0002988) and Inha University Grant. Also this work was supported by KIST Program (2E22760).

References

1. Shen W, Wang CY, Wang XH and Fu ZX: Oncolytic adenovirus mediated Survivin knockdown by RNA interference suppresses human colorectal carcinoma growth in vitro and in vivo. J Exp Clin Cancer Res 28: 81, 2009.
2. Potter JD: Colorectal cancer: molecules and populations. J Natl Cancer Inst 91: 916-932, 1999.
3. Oh BY, Lee RA and Kim KH: siRNA targeting Livin decreases tumor in a xenograft model for colon cancer. World J Gastroenterol 17: 2563-2571, 2011.
4. Zhang N, Yin Y, Xu SJ and Chen WS: 5-Fluorouracil: mechanisms of resistance and reversal strategies. Molecules 13: 1551-1569, 2008.
5. Pullarkat ST, Stoehlmacher J, Ghaderi V, Xiong YP, Ingles SA, Sherrod A, Warren R, Tsao-Wei D, Groshen S and Lenz HJ: Thymidylate synthase gene polymorphism determines response and toxicity of 5-FU chemotherapy. Pharmacogenomics J 1: 65-70, 2001.
6. Manfredini S, Bazzanini R, Baraldi PG, Bonora M, Marangoni M, Simoni D, Pani A, Scintu F, Pinna E and Pisano L: Pyrazole-related nucleosides. 4. Synthesis and antitumor activity of some 1-tetrahydropyranyl-4-substituted pyrazoles. Anticancer Drug Des 11: 193-204, 1996.
7. Park HJ, Lee K, Park SJ, Ahn B, Lee JC, Cho H and Lee KI: Identification of antitumor activity of pyrazole oxime ethers. Bioorg Med Chem Lett 15: 3307-3312, 2005.
8. Lv PC, Li HQ, Sun J, Zhou Y and Zhu HL: Synthesis and biological evaluation of pyrazole derivatives containing thiourea skeleton as anticancer agents. Bioorg Med Chem 18: 4606-4614, 2010.

9. Bandgar BP, Totre JV, Gawande SS, Khobragade CN, Warangkar SC and Kadam PD: Synthesis of novel 3,5-diaryl pyrazole derivatives using combinatorial chemistry as inhibitors of tyrosinase as well as potent anticancer, anti-inflammatory agents. Bioorg Med Chem 18: 6149-6155, 2010.
10. Christodoulou MS, Liekens S, Kasiotis KM and Haroutounian SA: Novel pyrazole derivatives: synthesis and evaluation of anti-angiogenic activity. Bioorg Med Chem 18: 4338-4350, 2010.
11. Fan C, Su H, Zhao J, Zhao B, Zhang S and Miao J: A novel copper complex of salicylaldehyde pyrazole hydrazone induces apoptosis through up-regulating integrin beta4 in H322 lung carcinoma cells. Eur J Med Chem 45: 1438-1446, 2010.
12. Calhelha RC, Ferreira IC, Peixoto D, Abreu RM, Vale-Silva LA, Pinto E, Lima RT, Alvelos MI, Vasconcelos MH and Queiroz MJ: Aminodi(hetero)arylamines in the thieno[3,2-b] pyridine series: synthesis, effects in human tumor cells growth, cell cycle analysis, apoptosis and evaluation of toxicity using non-tumor cells. Molecules 17: 3834-3843, 2010.
13. Pracharova J, Zerzankova L, Stepankova J, Novakova O, Farrer NJ, Sadler PJ, Brabec V and Kasparkova J: Interactions of DNA with a new platinum(IV) azide dipyridine complex activated by UVA and visible light: relationship to toxicity in tumor cells. Chem Res Toxicol 25: 1099-1111, 2010.
14. Weidner N, Semple JP, Welch WR and Folkman J: Tumor angiogenesis and metastasis - correlation in invasive breast carcinoma. N Engl J Med 324: 1-8, 1991.
15. Cristi E, Perrone G, Toscano G, Verzi A, Nori S, Santini D, Tonini G, Vetrani A, Fabiano A and Rabitti C: Tumour proliferation, angiogenesis, and ploidy status in human colon cancer. J Clin Pathol 58: 1170-1174, 2005.
16. Chen JM, Li WH, Wang JD, Feng YD, Wu JH and Gong JP: Cell balance between apoptosis and proliferation in colon cancer and its correlation with prognosis. Ai Zheng 24: 554-558, 2005 (In Chinese).
17. Esposito E and Cuzzocrea S: New therapeutic strategy for Parkinson's and Alzheimer's disease. Curr Med Chem 17: 2764-2774, 2010.
18. El-Deeb IM and Lee SH: Design and synthesis of new potent anticancer pyrazoles with high FLT3 kinase inhibitory selectivity. Bioorg Med Chem 18: 3961-3973, 2010.
19. Schmitz I, Kirchhoff S and Krammer PH: Regulation of death receptor-mediated apoptosis pathways. Int J Biochem Cell Biol 32: 1123-1136, 2000.
20. Igney FH and Krammer PH: Death and anti-death: tumour resistance to apoptosis. Nat Rev Cancer 2: 277-288, 2002.
21. Soengas MS, Capodieci P, Polsky D, Mora J, Esteller M, Opitz-Araya X, McCombie R, Herman JG, Gerald WL and Lazebnik YA: Inactivation of the apoptosis effector Apaf-1 in malignant melanoma. Nature 409: 207-211, 2001.
22. Nagane M, Levitzki A, Gazit A, Cavenee WK and Huang HJ: Drug resistance of human glioblastoma cells conferred by a tumor-specific mutant epidermal growth factor receptor through modulation of Bcl-XL and caspase-3-like proteases. Proc Natl Acad Sci USA 95: 5724-5729, 1998.
23. Pitti RM, Marsters SA, Lawrence DA, Roy M, Kischkel FC, Dowd P, Huang A, Donahue CJ, Sherwood SW and Baldwin DT: Genomic amplification of a decoy receptor for Fas ligand in lung and colon cancer. Nature 396: 699-703, 1998.
24. Xu X, Zhang Y, Qu D, Jiang T and Li S: Osthole induces G2/M arrest and apoptosis in lung cancer A549 cells by modulating PI3K/Akt pathway. J Exp Clin Cancer Res 30: 33, 2011.
25. Yang CJ, Wang CS, Hung JY, Huang HW, Chia YC, Wang PH, Weng CF and Huang MS: Pyrogallol induces G2-M arrest in human lung cancer cells and inhibits tumor growth in an animal model. Lung Cancer 66: 162-168, 2009.
26. Carmeliet P, Dor Y, Herbert JM, Fukumura D, Brusselmans K, Dewerchin M, Neeman M, Bono F, Abramovitch R and Maxwell P: Role of HIF-1alpha in hypoxia-mediated apoptosis, cell proliferation and tumour angiogenesis. Nature 394: 485-490, 1998.
27. Bolat F, Haberal N, Tunali N, Aslan E, Bal N and Tuncer I: Expression of vascular endothelial growth factor (VEGF), hypoxia inducible factor 1 alpha (HIF-1alpha), and transforming growth factors beta1 (TGFbeta1) and beta3 (TGFbeta3) in gestational trophoblastic disease. Pathol Res Pract 206: 19-23, 2010.
28. Spano D and Zollo M: Tumor microenvironment: a main actor in the metastasis process. Clin Exp Metastasis 29: 381-395, 2012.
29. Tao BB, Zhang CC, Liu SY and Zhu YC: Involvement of HIF-1 in the migration-promoting effects of hydrogen sulfide in vascular endothelial cells under normoxic conditions. Sheng Li Xue Bao 64: 129-134, 2012 (In Chinese).
30. Ergun S, Kilic N, Wurmbach JH, Ebrahimnejad A, Fernando M, Sevinc S, Kilic E, Chalajour F, Fiedler W and Lauke H: Endostatin inhibits angiogenesis by stabilization of newly formed endothelial tubes. Angiogenesis 4: 193-206, 2001.